The Journal of Experimental Biology 203, 3381–3390 (2000)
Printed in Great Britain © The Company of Biologists Limited 2000
JEB2888

MORPHOMETRIC PARTITIONING OF RESPIRATORY SURFACES IN AMPHIOXUS (*BRANCHIOSTOMA LANCEOLATUM* PALLAS)

ANKE SCHMITZ, MAJ GEMMEL AND STEVEN F. PERRY*

Institut für Zoologie, Rheinische Friedrich-Wilhelms-Universität Bonn, Poppelsdorfer Schloss, 53115 Bonn, Germany

*Author for correspondence (e-mail: perry@uni-bonn.de)

Accepted 21 August; published on WWW 24 October 2000

Summary

The anatomical diffusing factors (ADFs), defined as the ratio of surface area to the thickness of the diffusion barrier, of possible respiratory surfaces of adult amphioxus (*Branchiostoma lanceolatum*) were evaluated using stereological methods. The ADF is greatest for the lining of the atrium and for the skin covering the segmental muscles. Calculation of the diffusing capacities for O_2 revealed that the lining of the atrium makes up nearly 83 % of the entire diffusing capacity (8.86×10^{-3} μl min^{-1} mg^{-1} kPa^{-1}) while the skin over the segmental muscles (9 %), the skin over the metapleural fold (4 %) and the gill bars (4 %) are of minor importance. The diffusing capacity of surfaces lying over coelomic cavities makes up 76 % of the whole diffusing capacity, which is consistent with the hypothesis that the coelom may function as a circulatory system for respiratory gases. Muscles have approximately 23 % of the entire diffusing capacity, indicating that they may be self-sufficient for O_2 uptake. The diffusing capacity of the blood vessels in the gill bars is only 1 % of the total. Thus, the 'gills' lack significant function as respiratory organs in amphioxus (lancelets).

Key words: amphioxus, *Branchiostoma lanceolatum*, anatomical diffusing factor, diffusing capacity, oxygen uptake, respiratory organ, lancelet.

Introduction

The cephalochordates have recently gained increased credibility as the sister group of the craniates (Holland et al., 1996). One main difference between these groups remains the function of the branchial basket. In craniates, including the filter-feeding ammocetes larvae of lampreys, the gills are the main respiratory organ. The craniate gill structure is radically different from the ciliated gill bars of amphioxus, and the question arises as to whether such a major structural conversion could have occurred in an organ that is necessary for such a vital function as respiration.

In tunicates, the branchial basket functions both in filter feeding and in respiration, and the early literature (Rolph, 1876; Franz, 1927; Drach, 1948) also postulates both roles in the Cephalochordata. However, the respiratory function of the gill bars has been questioned, and even the terminology distances itself from any implication of respiratory function, calling these structures 'pharyngeal bars' (Orton, 1913; Rähr, 1979; Young, 1981; Gans, 1996). Detailed investigations of the respiratory system of amphioxus, however, are few and there is no consensus concerning the non-gill respiratory pathway. Rogers (1989) and Romer and Parsons (1977) assume that amphioxus breathes mainly *via* the skin of the entire body surface, while other authors suggest that the skin and the gill bars (Kent and Miller, 1997; Storch and Welsch, 1999), the skin of the metapleural fold (Young, 1981), the dorso-lateral atrial epithelium (Rähr, 1979) or the extensive coelomic spaces adjacent to the atrium (Orton, 1913) are the main sites of gas exchange. A quantitative morphological study that could answer the question regarding the possible sites of gas exchange has not been conducted to date.

A second question is that of the importance of the circulatory system in gas exchange. A central pump (heart) is lacking, but some vessels are secondarily motile because of the slow contraction of the myoepithelial lining of adjacent coelomic cavities (Rähr, 1981). Because these contractions appear not to be coordinated (Rähr, 1979; Young, 1981), and because amphioxus lacks endothelium, erythrocytes and respiratory pigments (Rähr, 1981), the vascular system seems to be not very effective in the circulation of respiratory gases. Thus, the importance of diffusion rather than of circulation for the transport of respiratory gases has been stressed (Gans, 1996).

In contrast to the circulatory system, the coelomic cavities of amphioxus are extensive and contain contractile myoepithelial cells (Welsch, 1975). Moreover, it is striking that the muscles and coelomic cavities lie adjacent to the outer (skin) and inner (epithelial lining of the atrium) body surfaces. This position would predispose these contractile tissues and fluid-filled spaces to direct gas exchange with the respiratory medium. Thus, the coelomic system may be the real circulatory system for respiratory gases, and the locomotor muscles may be self-sustaining.

Here, we use stereological morphometric methods to test the following hypotheses: (i) that the gill bars are of primary importance for respiration, and (ii) that the coelomic cavities, rather than the blood-vascular system, function as the circulatory system for gas transport.

Materials and methods

Experimental animals

Adult amphioxus (*Branchiostoma lanceolatum* Pallas) from the North Sea were provided by the Biologische Anstalt Helgoland (Germany) and maintained at 10 °C in North Sea water.

Histology

Twelve amphioxus of similar size were weighed, cold-anaesthetised and immersed in glutaraldehyde (2.5 % glutaraldehyde in 0.2 mol l^{-1} cacodylate buffer, pH 7.3, 4 °C; according to Stach and Eisler, 1998). The samples were fixed overnight, washed in buffer and postfixed with 1.5 % OsO_4 in the same buffer for 2 h at 0 °C. After washing in buffer, the samples were contrasted *en bloc* for 2 h with 0.5 % uranyl acetate in 0.05 mol l^{-1} maleic acid (pH 5). The samples were then dehydrated through an ethanol series, cut transversely into 12 pieces (see below) and embedded in Epon 812. The semi-thin sections (1.0 μm) were stained with 0.05 % Toluidine Blue in 0.05 % borax. For the stereological evaluation of the semi-thin sections, we used a light microscope with a drawing tube and a light box on which we placed our test array (Perry et al., 1994).

Volume determination: Cavalieri principle

The volume of the stereologically evaluated specimens was determined using the Cavalieri principle (Michel and Cruz-Orive, 1988), which estimates volume as the total cross-sectional area multiplied by the distance between the sections. For this purpose, just prior to embedding, each animal was cut into 12 pieces of equal length (*T*) (Fig. 1). Portions cranial to the first section and caudal to the last section were defined as comprising a single piece. The location of the first (starting) section was chosen randomly within an interval of *T*. Semi-thin sections were made of the cranial side of each piece. The areas of the sections were evaluated by point-counting at a final magnification of 144×, and volumes were calculated by multiplying the summed areas by *T*. The volumes of different organs, as a percentage of the total volume, were evaluated by point-counting.

Surface areas and barrier thickness: vertical sections

For evaluation of surface areas and barrier thickness, we used the vertical section method (Baddeley et al., 1986) (Fig. 1). The sagittal plane of the animals was defined to be the

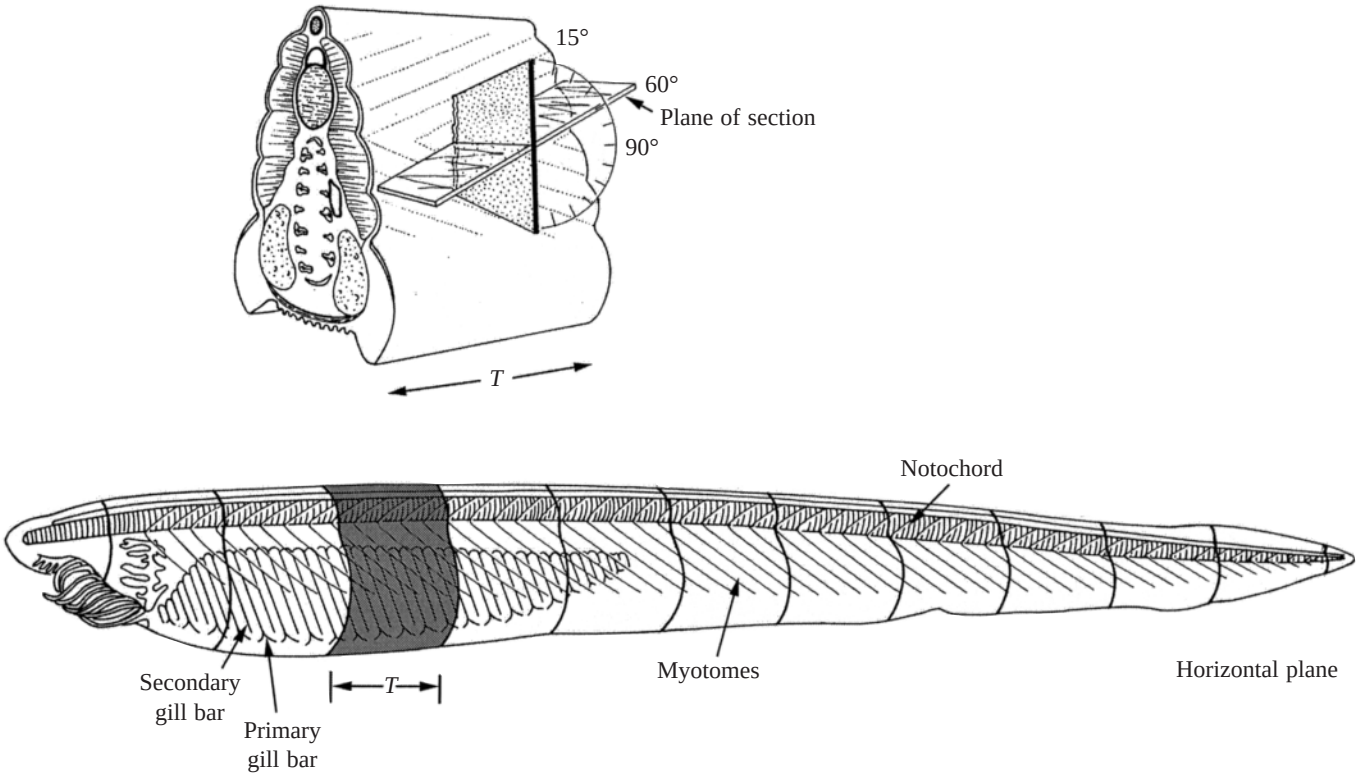

Fig. 1. Schematic drawing of *Branchiostoma lanceolatum* demonstrating the sampling methods for the Cavalieri principle, and the vertical section method. For the Cavalieri principle, animals were cut transversely into 12 pieces of equal length (*T*). For the vertical sections (enlarged slice), the plane of section was in the vertical axis, the horizontal plane being the sagittal plane of the animal. One example (60 ° from the starting direction) is given in the enlarged slice. See text for further details.

horizontal plane; vertical planes were all planes perpendicular to the horizontal plane. After making the transverse sections for volume determination, we re-embedded the tissue pieces of the 12 specimens according to the systematic random sampling method (Gundersen and Jensen, 1987). The pieces were rotated sequentially about the axis of the vertical planes, starting at a randomly chosen angle within 0–15° from the original orientation for the first piece and adding 15° for each further piece. The depth of the section within the tissue block was also chosen at random. The data were pooled and evaluated for the entire group of 12 amphioxus (Howard and Reed, 1998).

The surface areas of (i) the skin over the trunk muscles, (ii) the skin over the metapleural fold, (iii) the gill bars and (iv) the atrium were determined from their respective surface-area-to-volume ratios (S_V) multiplied by the volume of the whole animals. The S_V of each component was determined by point- and intersection-counting (for the test array, see Fig. 3E) of the semi-thin sections at a final magnification of 144×, moving the test grid systematically over the sections and evaluating every third test field. S_V was calculated as $S_V=2I/L$, where I is the number of intersections of the test lines with the surface and L is the total length of test lines. Respiratory surface areas (S_R) were evaluated during measurements of barrier thickness (Figs 2, 3A–D) and are defined as those surfaces exposed to respiratory medium that are not connected by a measurement line to another such surface. Points connected with measurement lines that left the field of measurement were not counted. The percentage of a surface area that is respiratory (%S_R) was calculated as $100p_R/(p_R+p_{NR})$, where p_R and p_{NR} are points falling on respiratory and non-respiratory surfaces, respectively.

Barrier thickness was measured at the light microscopic level with a half-logarithmic ruler in randomly chosen directions (Perry, 1981). The starting point of a measurement was selected in an unbiased way by the test array (Fig. 3E). The following structures were measured (Figs 2, 3A–D): (i) the thickness of the skin over lateral trunk muscles (final magnification 375×), (ii) the thickness of the skin over the metapleural fold (144×), (iii) the thickness of the skin over ventral muscle (144×) (for i–iii, these were defined as distances from water to coelomic cavities or to muscles), (iv) the water–blood distance in the gill bars (distances from water to blood vessels) (375×), (v) the water–coelom distance in the gill bars (375×) and (vi) the thickness of the atrial epithelium [the distances from water to muscles and to the coelomic cavities of (a) the gonads, (b) the gut and (c) the subchordal coelom] (600×).

The harmonic mean lengths of the measured distances were calculated as:

$$l = \frac{N}{\sum_{i=1}^{N} \frac{1}{l}},$$

where N is the number of measuring points and l is the harmonic mean length, calculated from the individual measured lengths l_i. l was then converted to the harmonic mean barrier thickness as $\tau=\frac{2}{3}l$ (Weibel and Knight, 1964). According to Fick's first law, thin regions are more relevant for gas exchange than are thick regions. Therefore, the harmonic mean, which weights in favour of small values, is more relevant than is the arithmetic mean. In the mathematical derivation for the determination from randomly oriented sections, the harmonic mean of measured lengths must be multiplied by the factor 2/3 to compensate for an overestimate due to the random orientation of the measured intercepts (Weibel and Knight, 1964).

The anatomical diffusion factors (ADFs; Perry, 1978) were calculated as the respiratory surface area in relation to body mass (S_R/M_B) divided by the harmonic mean barrier thickness (τ) of the respective layers.

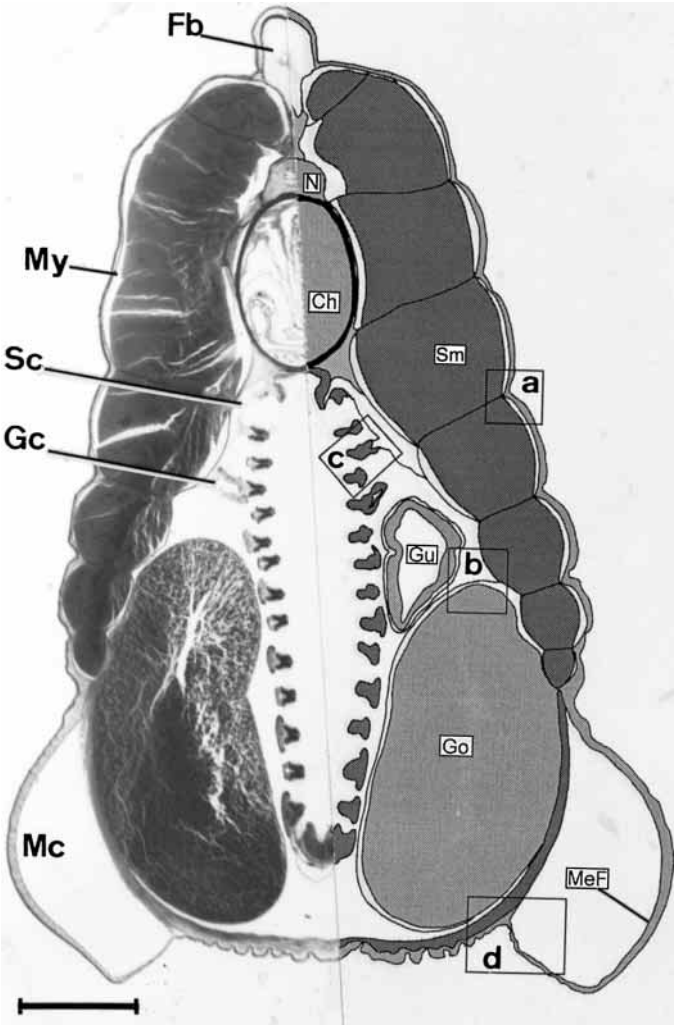

Fig. 2. Cross section of *Branchiostoma lanceolatum* in cranial view: a light micrograph is shown in the left half and a schematic drawing in the right half of the image. In the drawing, four regions (a–d) are marked that are illustrated as micrographs in Fig. 3A–D. Ch, chorda dorsalis; Fb, fin box; Gc, gill coelom; Go, gonad; Gu, mid-gut diverticulum; Mc, metapleural coelom; MeF, metapleural fold; Sm, segmental muscles; My, myocoel; N, notochord; Sc, subchordal coelom. Scale bar, 500 μm.

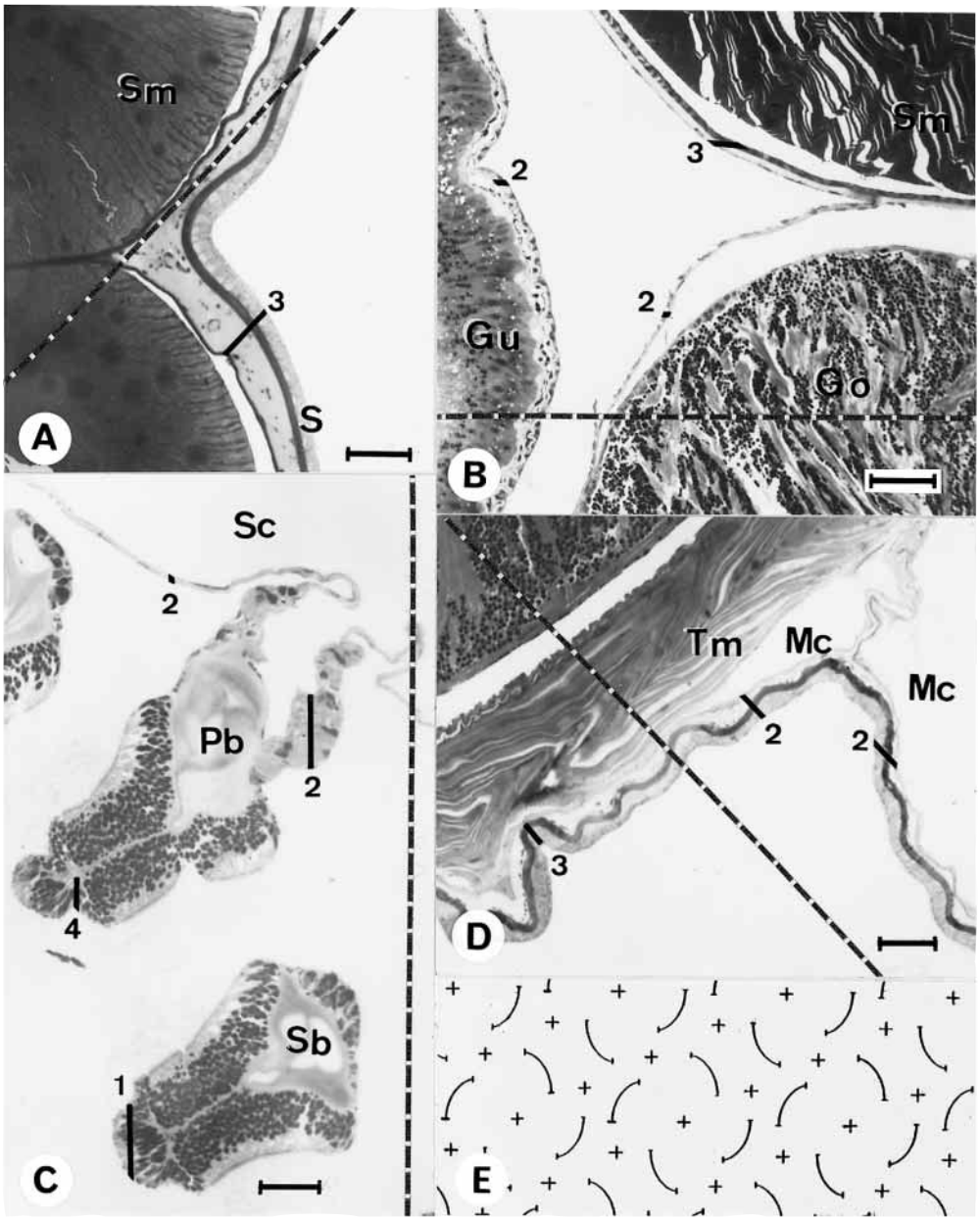

Fig. 3. (A–D) Light micrographs of the regions a–d marked in Fig. 2. Some examples are given for the measurement of barrier thickness. The directions of measurements are marked as dashed lines on entire pictures, and measurement lines parallel to the illustrated direction are marked in black. Numbers in A–D indicate types of measurements: 1, measurement line connecting water with water (non-respiratory surfaces); 2, measurement line connecting water with coelomic cavity; 3, measurement line connecting water with muscle (segmental muscles Sm in A and B, transverse muscle Tm in D); 4, measurement line connecting water with gill blood vessel. (A) Body wall and segmental muscles. S, skin. (B) Atrium near the mid-gut diverticulum (Gu), gonads (Go) and segmental muscles. (C) Part of the pharynx with primary gill bars (Pb), secondary gill bars (Sb) and a section of the subchordal coelom (Sc). (D) Part of the metapleural fold with metapleural coelom (Mc) and transverse muscle (Tm). Scale bars, 40 μm in A and B and 25 μm in C and D. (E) A portion of the test array that was superimposed on the microscopic image for the evaluation of the surface-area-to-volume-ratio and to determine the starting points of measurement lines for the barrier thickness. See text for further details.

The diffusing capacities were calculated as the product of the ADFs and Krogh's diffusion coefficient (K), corrected to 11 °C (Bartels, 1971). The skin over trunk muscles and the skin over metapleural folds is composed of four different layers: (i) epidermis (ep), (ii, iii) two layers of connective tissue (ct); and (iv) a gelatinous layer (ge) with blood vessels, nerves and coelomic cavities. For connective tissue, we used the corrected, published value for frog connective tissue (K=10.38×10^{-8} cm^2 min^{-1} kPa^{-1}), for the gelatinous layer that of gelatine (K=25.19×10^{-8} cm^2 min^{-1} kPa^{-1}) and for the epidermis that of rat lung tissue (K=18.27×10^{-8} cm^2 min^{-1} kPa^{-1}). The diffusing capacity of the skin (D_{Sk}) over the lateral muscles and metapleural folds is calculated as the reciprocal of the sum of the reciprocal values of the diffusing capacities of the different layers (D_{ep}, D_{ct} and D_{ge}, respectively) (Weibel, 1970/71), according to their proportions, evaluated by simple point-counting measurements: $1/D_{Sk}=1/D_{ep}+1/D_{ct}+1/D_{ge}$.

Statistical analyses

To evaluate the estimator variance, we calculated the standard deviation (S.D.) and coefficient of error (C.E.) of our barrier thickness measurements. Because the thickness of the barrier τ is calculated from the harmonic mean of the intercept lengths and the standard deviation for the harmonic mean is not defined, we calculated the standard deviation and coefficient of error of the arithmetic mean of the intercept lengths. As the S_V values were evaluated at every third test field, we calculated the estimator variance of S_V as the standard deviation and coefficient of error of the values of intersections (I) and points (P) of those fields that were sampled (see

Fig. 3E; *I* is the intersection of a cycloid arc with the surface and *P* is the centre of a cross falling over a structure).

For the Cavalieri principle, the precision of the estimate (the total variance of the counted points or var*P*) depends on the noise (inaccuracy of the test array) and the variance of the sum of the areas ($var_{\sum area}$):var*P*=noise+$var_{\sum area}$ (Gundersen and Jensen, 1987; Howard and Reed, 1998). The noise indicates how much the estimate could change if the test array were placed differently. It is calculated as: $0.0724(b\sqrt{a})\sqrt{(n\sum P)}$, where $b\sqrt{a}$ is the 'average profile shape' (5 in our case), *n* is the number of sections, and $\sum P$ is the sum of all counted points. The variance of the area is a function of the number of sections, and calculation is based on a covariogram analysis of data from cross-sectional areas (Howard and Reed, 1998).

The coefficient of error is calculated from var*P* and the sum of all counted points according to: $C.E.(\sum P)=\sqrt{(varP)}/\sum P$ (Cruz-Orive, 1993; Howard and Reed, 1998).

Rates of O_2 consumption (respirometry)

The rates of O_2 consumption of eight adult amphioxus were measured using a Gilson differential respirometer. The measurement interval extended over a period of 6–7 h in the light (observation intervals 15 min). Animals were measured in 40 ml flasks, the bottom covered with amphioxus sand, in sea water with bactericidal medium (Baktopur, Sera). The experiments were carried out at 11 °C, and 10 % KOH was placed in the centre well of the flasks to absorb the CO_2. Rates of O_2 consumption were converted to volume of O_2 utilized per unit time per milligram tissue ($\mu l\,h^{-1}\,mg^{-1}$) at STPD.

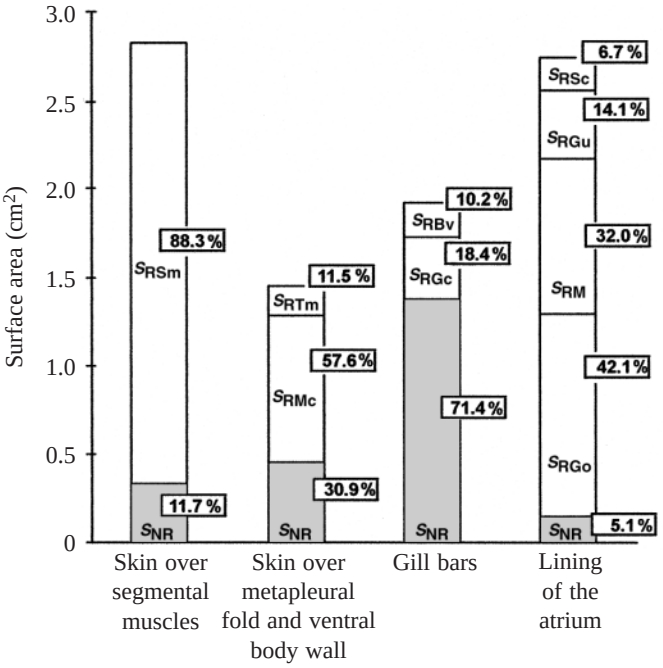

Fig. 4. Respiratory (S_{Rx}) and non-respiratory (S_{NR}) surfaces of the four body regions, where *x* is one of the following subscripts: Bv, blood vessel; Go, gonocoel; Gc, gill coelom; Gu, gut coelom; M, muscles (segmental and transverse); Mc, metapleural coelom; Sc, subchordal coelom; Sm, segmental muscle; Tm, transverse muscle. Values are given for one hypothetical amphioxus of body mass 217 mg.

Results

Volumetry, surface area and ADF

The mean body mass of the 12 stereologically evaluated amphioxus was 0.217±0.04 g (mean ± S.D., range 0.152–0.279 g) and the mean volume was 0.204±0.04 cm^3 (0.151–0.266 cm^3). The volume of muscles was 40.1 %, that of the gut and gonads 16 %, that of the coelomic cavities 8.6 % and that of the gill bars 2.7 % of the entire animal (C.E. 2.7–3.7 %).

Values for surface areas represented by inner surfaces (lining of the atrium 31 %, and gill bars 21 %, of the entire surface area) and outer surfaces (skin over trunk muscles 32 %, and skin over metapleural fold 16 %, of the entire surface area) are shown in Fig. 4. The percentages of these respiratory surfaces represented by the different regions evaluated are also shown in Fig. 4. For gill bars, S_R is only 28.6 % of the entire gill surface, while for the skin over the trunk muscles (88.3 %), for the skin over the metapleural fold (69.1 %) and for the atrial epithelium (94.9 %) the $\%S_R$ is clearly greater.

Stereologically evaluated values for the respiratory surface area, barrier thickness and anatomical diffusing factors (ADF) of potential respiratory surfaces, calculated for a single amphioxus of body mass (M_B) 217 mg (the mean M_B in this study), are summarised in Table 1. The respiratory surface area is greatest for the atrial epithelium (2.6 cm^2) and for the skin over the trunk muscles (2.5 cm^2), while the respiratory surface of the gill bars is only 0.55 cm^2. The respiratory surface area of all surfaces covering muscles is 3.54 cm^2, and for all surfaces with direct contact to coelomic cavities it is 2.91 cm^2.

The diffusing barrier is thickest for distances connecting (i) water and coelom and (ii) water and muscles in the skin over the lateral muscles and over the metapleural folds. In the gill bars, the diffusing barriers that allow gas exchange between water and blood vessels or between water and coelomic cavities are 17.6 and 12.9 μm, respectively. The diffusing barrier of the lining of the atrium (atrial epithelium and coelothelium over coelomic cavities or atrial epithelium and basal laminae over muscles) is between 2 and 6 μm and is, therefore, thinner by a factor of 3–11 than the values for the other potential respiratory surfaces (Table 1).

The ADF is greatest for the lining of the atrium connected by measuring lines with coelomic cavities surrounding the gonads (24 455 $cm\,g^{-1}$) followed by the ADFs of inner surfaces over muscles, the skin over the trunk muscles and the remaining coelomic cavities (Table 1). The ADF of the gill bars amounts to 1259 $cm\,g^{-1}$ for coelomic cavities and to 514 $cm\,g^{-1}$ for blood vessels.

Diffusing capacities

Diffusing capacities (Table 2) were clearly greatest for the lining of the atrium (7.43×10^{-3} $\mu l\,min^{-1}\,kPa^{-1}\,mg^{-1}$) and for

Table 1. *Stereological evaluated values for barrier thickness, respiratory surface area and anatomical diffusing factor*

Structure		Respiratory surface area, S (cm^2)	Respiratory surface area/body mass, M ($cm^2\ g^{-1}$)	Diffusing barrier, τ (μm)	ADF ($cm\ g^{-1}$)
Skin over segmental muscles		2.49	11.51	22.46	5 124
Skin over metapleural fold		1.04	4.81		
	Metapleural coelom	0.83	3.85	28.79	1 337
	Transversal muscle	0.17	0.77	18.78	409
Gill bars		0.55	2.54		
	Gill coelom	0.35	1.63	12.92	1 259
	Gill blood vessels	0.20	0.91	17.61	514
Lining of the atrium		2.61	12.03		
	Subchordal coelom	0.18	0.85	2.03	4 185
	Gonocoel	1.16	5.33	2.18	24 455
	Gut coelom	0.39	1.79	3.35	5 348
	Muscles	0.88	4.06	6.08	6 677

ADF, anatomical diffusing factor [$S/(M\tau)$].
Values are given for one hypothetical amphioxus of 217 mg body mass (the mean body mass of the 12 specimens evaluated).

surfaces over coelomic cavities ($6.69\times10^{-3}\ \mu l\ min^{-1}\ kPa^{-1}\ mg^{-1}$). The diffusing capacity for all inner and outer surfaces covering muscles is $2.08\times10^{-3}\ \mu l\ min^{-1}\ kPa^{-1}\ mg^{-1}$, while it is only $0.09\times10^{-3}\ \mu l\ min^{-1}\ kPa^{-1}\ mg^{-1}$ for the blood vessels of the gill bars. The total diffusing capacity for one amphioxus is $8.86\times10^{-3}\ \mu l\ min^{-1}\ kPa^{-1}\ mg^{-1}$ or $1.922\ \mu l\ min^{-1}\ kPa^{-1}$ for a 217 mg specimen.

Rates of O_2 consumption

The rate of O_2 consumption ($\dot{M}_{O_2}$) of the eight animals examined (M_B=149±22.7 mg, mean ± S.D., range 121.9–191.3 mg) was between 0.026 and 0.037 $\mu l\ h^{-1}\ mg^{-1}$, giving a mean $\dot{M}_{O_2}$ of 0.0325±0.004 $\mu l\ h^{-1}\ mg^{-1}$ (at STPD), or 4.83±0.68 $\mu l\ h^{-1}$ (STPD) for a 149 mg specimen (Fig. 5).

Discussion

Methods

Fixation for microscopy was carried out in buffer of osmolarity near that of sea water, and the tissue was embedded in epoxy resin, thus minimising shrinkage or swelling. Stereological estimates are normally performed on isotropic uniform random sections of pooled samples or, as in the present case, on vertical sections of individual animals. Using vertical sections, the variance among animals will differ systematically according to the plane of sectioning. Thus, and because we used pooled samples, we could not determine the between-animal variance, but it is generally assumed to be approximately 15 % of the mean (L. M. Cruz-Orive, personal communication). The coefficient of error (C.E.) of all measured values lies far below 15 % (Table 3). Therefore, the observed variation in volumes, surface areas, barrier thicknesses and ADF is dominated by the biological variation.

The calculated diffusing capacities are only estimates and could be in error because the values for Krogh's diffusion constant (K) employed might differ from those of amphioxus tissue. The similarity of K values for similar tissue types from different animals (Bartels, 1971), however, suggests that the present estimates are reasonable. In addition, dynamic processes such as convective movement of the water, blood and coelomic fluid were not considered. Thus, the physiological diffusing capacity ($\dot{M}_{O_2}/\Delta P_{O_2}$) may differ substantially from the present morphometric estimate.

Table 2. *Diffusing capacities of the structures evaluated*

		Diffusing capacity ($\mu l\ min^{-1}\ kPa^{-1}\ mg^{-1}$)
Skin over segmental muscles		0.78×10^{-3}
Skin over metapleural fold		0.32×10^{-3}
	Metapleural coelom	0.25×10^{-3}
	Transversal muscle	0.08×10^{-3}
Gill bars		0.32×10^{-3}
	Gill coelom	0.23×10^{-3}
	Gill blood vessels	0.09×10^{-3}
Lining of the atrium		7.43×10^{-3}
	Subchordal coelom	0.76×10^{-3}
	Gonocoel	4.47×10^{-3}
	Gut coelom	0.98×10^{-3}
	Muscles	1.22×10^{-3}

Values taken for Krogh's diffusion coefficient (K) are: connective tissue, $10.38\times10^{-8}\ cm^2\ min^{-1}\ kPa^{-1}$ (from connective tissue of frog); gelatinous layers, $25.19\times10^{-8}\ cm^2\ min^{-1}\ kPa^{-1}$ (gelatine); epidermal layers, $18.27\times10^{-8}\ cm^2\ min^{-1}\ kPa^{-1}$ (from rat lung tissue) (Bartels, 1971).

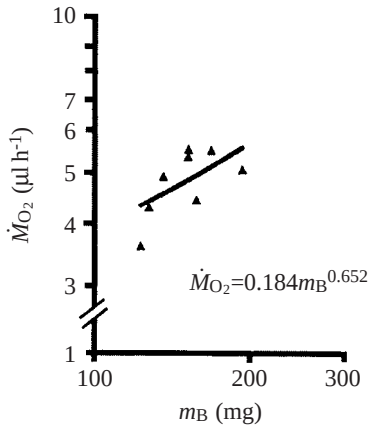

Fig. 5. Double logarithmic diagram of the rate of oxygen consumption ($\dot{M}_{O_2}$) of eight *Branchiostoma lanceolatum* at 11 °C plotted against body mass (M_B) at STPD, r^2=0.46, P<0.05.

Rates of O_2 consumption

We assume that we measured resting rates of O_2 consumption because the sea water used contained no food particles and the animals did not swim in the vessels. Inactivity might also be due to the low temperatures used in our experiments because *B. lanceolatum* is adapted to temperatures of 10–25 °C (Courtney, 1975). We measured $\dot{M}_{O_2}$ at the low end of this range because the experiments were performed in March–May when the North Sea is still cold. Bactericidal agents were added to eliminate the possibility of microbial O_2 consumption during respirometry. Inactive ammocetes of the lamprey *Ichthyomyzon hubbsi* have a similar $\dot{M}_{O_2}$ (0.022 µl h^{-1} mg^{-1}, 9.5 °C, animal mean mass 1.24 g) (Hill and Potter, 1970). An $\dot{M}_{O_2}$ of 0.0358 ml h^{-1} g^{-1} at 16 °C for *B. lanceolatum* was reported by Nicol (1960). Bishop et al. (1998) measured 0.08–0.18 ml h^{-1} g^{-1} for *B. californiense* at 16 °C.

Courtney and Newell (1965) found a threefold increase in $\dot{M}_{O_2}$ above the resting value during feeding. Thus, the difference between the present values and those of Nicol (1960) *versus* the higher ones of Bishop et al. (1998) could indicate that our animals were in the resting (non-feeding) state.

Comparison of ADFs

The ADF is greatest for the coelomic cavities surrounding the gonads. This is due both to the large surface area of this structure, the greatest respiratory surface area evaluated for a single structure, and to the generally thin epidermal lining of the atrium. We only examined adult animals with well-developed gonads, which bulge into the atrium: the value for immature animals will certainly be smaller.

The gill bars provide a small respiratory surface area together with large diffusing barriers. As we did not include the diffusing barrier provided by the cilia themselves, the actual ADF values may be even lower than those calculated.

Comparison of diffusing capacities

Of the entire diffusing capacity, 87 % is provided by the inner respiratory surfaces (Fig. 6B). The skin over segmental muscles represents 70 % of the diffusing capacity of the outer

Table 3. *Statistics for measured line lengths and surface-area-to-volume ratios*

		Mean (µm)	S.D.	C.E. (%)	Number of measurements
Line length, l_i					
Skin over segmental muscles		39.32	15.59	1.1	1300
Skin over metapleural fold	Metapleural coelom	67.83	44.40	1.4	2305
	Transversal muscle	45.11	36.92	3.8	460
Gill bars	Gill coelom	33.42	21.23	1.8	1180
	Gill blood vessels	33.38	15.85	1.9	657
Lining of the atrium	Subchordal coelom	4.49	3.79	4.9	296
	Gonocoel	5.19	5.69	3.8	835
	Gut coelom	7.38	5.48	4.0	340
	Muscles	13.88	9.96	2.8	670

Intersections (I) and points (P) for determination of S_V	Total number of I or P (unitless)	Mean (unitless)	S.D.	C.E. (%)	Number of fields evaluated
Skin over segmental muscles (I)	1 149	1.6	1.7	4.1	743
Skin over metapleural fold (I)	589	0.8	1.6	7.6	743
Gill bars (I)	781	1.1	2.5	8.7	743
Lining of the atrium (I)	866	1.2	2.2	6.9	743
Points over all structures (P)	19 373	26.1	15.1	2.2	743

S_V, surface-area-to-volume ratio; C.E., coefficient of error; S.D., standard deviation.

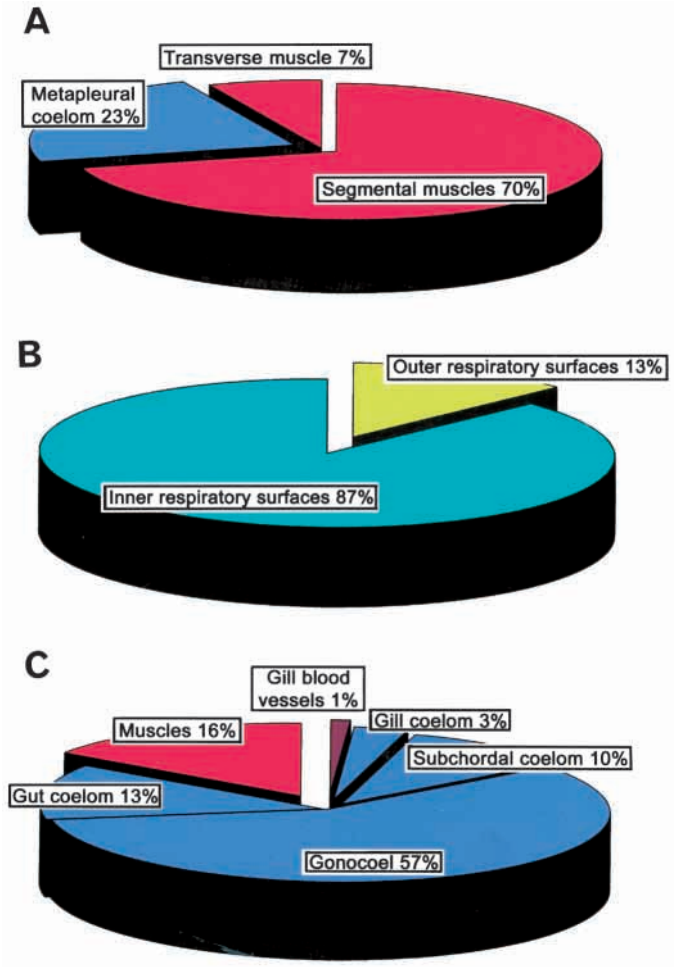

Fig. 6. Diffusing capacities of respiratory surfaces. (A) Partitioning of the outer surfaces. (B) Partitioning of the outer and inner surfaces. (C) Partitioning of the inner surfaces.

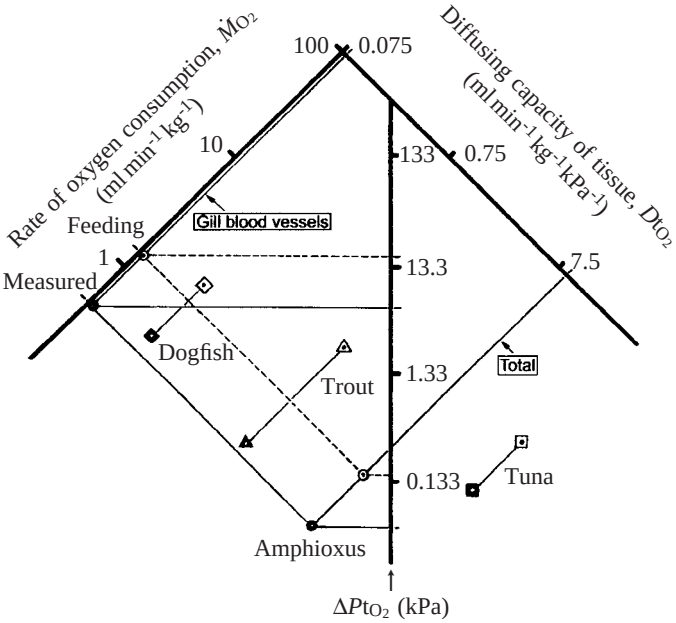

Fig. 7. Double logarithmic plot demonstrating the driving pressure for O_2 diffusion (ΔP_{tO_2};kPa) ($\dot{M}_{O_2}/D_{tO_2}=\Delta P_{tO_2}$) (read perpendicularly against the central axis) as a combination of the rate of oxygen consumption ($\dot{M}_{O_2}$) and the morphological diffusing capacity of tissue (D_{tO_2}), each read perpendicularly against the respective axis. For comparison, values for some fishes are given. For each species, the filled symbols represent the resting values, and the open symbols represent maximum $\dot{M}_{O_2}$ (feeding for amphioxus and exercising for fishes). For amphioxus feeding, $\dot{M}_{O_2}$ values are estimated to be three times our measured value. For sources of values for fishes (trout, *Oncorhynchus mykiss*; tuna, *Thunnus albacares*; dogfish, *Scyliorhinus canicula*), see Perry (1990).

respiratory surfaces (Fig. 6A). For the inner surfaces (Fig. 6C), more than half of the diffusing capacity is provided by the surface of the coelomic cavities surrounding the gonads, while the other surfaces of the atrium share most of the remaining diffusing capacity with the gill bars providing only 4 %. With regard to the O_2 diffusion pathway, 76 % of the diffusing capacity leads to coelomic cavities, 23 % directly to muscles and only 1 % to the blood vessels of the gill bars.

An indicator of the degree to which respiratory organs are exploited is the rate of O_2 consumption ($\dot{M}_{O_2}$) per unit diffusing capacity of the respiratory tissue in contact with water (D_{tO_2}) (Fig. 7). This factor has the units (kPa) of the driving pressure for O_2 (ΔP_{tO_2}) in Fick's first law. Inspection of Fig. 7 shows that the $\dot{M}_{O_2}$ of a filter-feeding amphioxus combined with the total diffusing capacity of the animal results in a ΔP_{tO_2} that is comparable with that of quiescent teleosts. If only the blood vessels of the gill bars are considered, however, the resulting mean driving pressure would be in excess of 13.3 kPa, meaning that the gills would have to be as efficient as those of a teleost, which are able to extract over 80 % of the dissolved O_2 from the water (Marshall and Hughes, 1980). This is highly unlikely in the light of the lack of countercurrent exchange and haemoglobin in amphioxus, and also considering that the ciliary pump may consume much of the O_2 passing over it. The ΔP_{tO_2} value for the exercising dogfish shark (*Scyliorhinus canicula*), while high for a fish, is only half that of amphioxus gills.

How does amphioxus breathe?

Our results refute the hypothesis that the gill bars are of major importance for respiration in amphioxus. This conclusion is supported by previous studies that emphasise the function of the gill basket in filter feeding (Orton, 1913; Riisgard and Svane, 1999). Orton (1913) suggests that because of the high rate of O_2 consumption of the cilia of the gill bars, blood may actually leave the gills less rich in O_2 than when it enters them. Considerable O_2 consumption by the gill bars was also emphasised by the findings of Baskin and Detmers (1976), who demonstrated mucus secretion not only at the endostyle but also at the pharyngeal margin of the gill bars.

If the gills do not function in O_2 uptake, other body regions must carry out this function. The atrium is constantly ventilated by the water current used for filter feeding, thus guaranteeing

a steady ΔP_{O_2}. All organs having contact with the lining of the atrium (gonads, gut, segmental muscles and transverse muscle, gill bars) might therefore be self-sufficient in O_2 uptake and also in CO_2 release.

Muscles could additionally take up O_2 *via* the skin. According to Holland and Holland (1990), there is a myocoel between the skin and the trunk muscles, which would increase the coelomic proportion of the diffusing capacity. During times of little convection of sea water, e.g. when the animals are buried in the sand, little movement of the myocoel contents would be expected. Swimming activity, however, would result in convection just when the muscles require large amounts of O_2. In this context, it is of interest that amphioxus show different behaviour in different substrata: they tend to lie on top of dense, muddy substrata, but they burrow deeply into coarse sand (Webb and Hill, 1958). This behaviour could be due to the relative availability of oxygenated water for the outer respiratory surfaces (skin).

The circulatory system of amphioxus seems poorly adapted for the transport of respiratory gases because respiratory pigments are lacking (Rähr, 1981), and blood flows slowly and undergoes changes in flow direction (Wolf, 1941; Azariah, 1965; Rähr, 1981). The present study implies that the blood passing through the gill bars cannot supply amphioxus with enough O_2 to support aerobic metabolism. Thus, to serve a respiratory function, blood vessels must lie in another respiratory epithelium such as the atrium or the skin, whence oxygenated blood can be transported to the consuming organs. Most blood vessels lack such direct contact with gas-exchanging surfaces. The epithelium of the gut and gonads is vascularised but, since the blood vessels lack contractile tissue, blood flow cannot be ensured. Thus, the gill vessels presumably serve to remove metabolic waste products from the ciliary apparatus to provide the nephridial filter organs with blood and to connect the dorsal and ventral parts of the circulatory system.

The respiratory surfaces covering muscles, atrial epithelium and skin over the trunk muscles do possess a plexus of endothelium-free blood spaces (Rähr, 1979, 1981). However, these blood vessels could only help in providing O_2 to the muscles if they anastomose with blood spaces that penetrate those muscles. While evidence for such a deep muscle network is lacking (Rähr, 1981), spaces connecting with the myocoel extend deep into the segmental muscles.

Unlike other coleomic cavities, the myocoel and sclerocoel lack a myoepithelial lining (Holland and Holland, 1990). This anatomical arrangement is consistent with the hypothesis that coelomic fluid perfuses the muscles during swimming movements at times of maximal O_2 consumption, thus supporting the contention of O_2 self-sufficiency of the segmental muscles. The same argument could apply to the notochord, which is located medial to the sclerocoel. Recently, haemoglobin was found in the notochord cells and myotome tissues in *B. californiense* (Bishop et al., 1998). This haemoglobin may be involved in facilitating O_2 delivery, perhaps directly through the skin. Thus, it provides an O_2 store to maintain a high level of aerobic metabolism in the organs that consume most O_2 during locomotor activity (Bishop et al., 1998).

For amphioxus larvae, it has been suggested that coelomic cavities may function as a vascular system at a stage when the blood vessels are rudimentary (Stach, 1998). We extend this model to the adult animal. In general, most coelomic cavities have close contact with respiratory surfaces, and it is possible that O_2 is taken up directly by the coelomic fluid and transported within the coelomic cavities and thence by diffusion into the tissues. This includes the coelom surrounding the gut and gonads as well as the cavities of the subchordal coelom and the metapleural fold. The coelomic fluid could transport O_2 by active contraction or by passive distortion of the coelomic cavities to deep body regions that lack direct contact with respiratory surfaces. The presence of a contractile myoepithelial lining in most coelomic cavities (Welsch, 1975) supports this model.

Physiological investigations providing measurements of the ΔP_{O_2} between the water and the coelomic cavities or blood vessels would further our understanding of which tissues serve respiratory functions in amphioxus.

Phylogenetic significance

The implications of the present study for a filter feeder as the common ancestor of amphioxus and vertebrates are intriguing. While not able to provide anatomical details of the transition to gill breathing, functional anatomical analyses such as this can point out functional constraints that could make one pathway of evolution more probable than another.

If, as in amphioxus, the atrial surface of the vertebrate ancestor rather than the gill bars themselves were the respiratory exchanger, then a stepwise modification of the gill structures can be envisioned. The ventilatory motor could be changed from cilia to a velum, and expanded surfaces could develop in the gills while leaving the filter-feeding mechanism intact, as in the ammocetes larva (Mallat, 1984). Such a major modification would be difficult to envision if the gills were the major respiratory organ. However, the rudiments of a vertebrate circulatory system are present, which, given an increased respiratory gill function, could supply the body tissues with O_2.

Furthermore, increasing the size and mineralization of the skin, as in early vertebrates, would place a greater demand on the respiratory pharynx: the segmental muscles would no longer be self-sufficient for gas exchange. Interestingly, this scenario also casts light on other mineralized animals, such as calcichordates (Jefferies and Jacobson, 1998). Having made the basic transition from filtering to a respiratory gill, the hypothetical vertebrate ancestor could then internalise the gonads and all other organ systems that had previously been wholly or partly self-sufficient of respiratory surfaces.

We thank Marion Schlich for preparing the photographs and Beatrice Ollenschlaeger for drawing Fig. 1.

References

Azariah, J. A. (1965). On the reversal of the heart beat in *Branchiostoma lanceolatum*. *J. Mar. Biol. Ass. India* **7**, 58–60.

Baddeley, A. J., Gundersen, H. J. and Cruz-Orive, L. M. (1986). Estimation of surface area from vertical sections. *J. Microsc*. **142**, 259–276.

Bartels, H. (1971). Diffusion coefficients and Krogh's diffusion constants. In *Respiration and Circulation* (ed. P. L. Altman and D. S. Dittmer), pp. 21–22. *Biological Handbooks*. Bethesda, MD: Federation of American Societies for Experimental Biology.

Baskin, D. G. and Detmers, P. A. (1976). Electron microscopic study on the gill bars of amphioxus (*Branchiostoma californiense*) with special reference to neurociliary control. *Cell Tissue Res*. **166**, 167–178.

Bishop, J. J., Vandergon, T. L., Green, D. B., Doeller, J. E. and Kraus, D. W. (1998). A high-affinity hemoglobin is expressed in the notochord of amphioxus, *Branchiostoma californiense*. *Biol. Bull*. **195**, 255–259.

Courtney, W. A. M. (1975). The temperature relationships and age-structure of North Sea and Mediterranean populations of *Branchiostoma lanceolatum*. *Symp. Zool. Soc. Lond*. **36**, 213–233.

Courtney, W. A. M. and Newell, R. C. (1965). Ciliary activity and oxygen uptake in *Branchiostoma lanceolatum* (Pallas). *J. Exp. Biol.* **43**, 1–12.

Cruz-Orive, L. M. (1993). Systematic sampling in stereology. *Bull. Int. Statist. Inst. Proc.* **49**, 451–468.

Drach, P. (1948). Embranchement des Céphalocordés. In *Traité de Zoologie XI* (ed. P.-P. Grassè), pp. 931–1037. Paris: Libraires de l'Academie de Médecine.

Franz, V. (1927). Morphologie der Akranier. *Z. Ges. Anat.* **27**, 464–692.

Gans, C. (1996). Study of the lancelets: The first 200 years. *Isr. J. Zool.* **42**, 3–11.

Gundersen, H. J. G. and Jensen, E. B. (1987). The efficiency of systematic sampling in stereology and its prediction. *J. Microsc*. **147**, 229–263.

Hill, B. J. and Potter, I. C. (1970). Oxygen consumption in ammocoetes of the lamprey *Ichthyomyzon hubbsi* Raney. *J. Exp. Biol*. **53**, 47–57.

Holland, N. D. and Holland, L. Z. (1990). Fine structure of the mesothela and extracellular materials in the coelomic fluid of the fin boxes, myocoels and sclerocoels of a lancelet, *Branchiostoma floridae* (Cephalochordata=Acrania). *Acta Zool*. **71**, 225–234.

Holland, N. D., Panganiban, G., Henyey, E. L. and Holland, L. Z. (1996). Sequence and developmental expression of *AmphiDII* and amphioxus *Distal-less* gene transcribed in the ectoderm, epidermis and nervous system: insights into evolution of craniate forebrain and neural crest. *Development* **122**, 2911–2920.

Howard, C. V. and Reed, M. G. (1998). *Unbiased Stereology, Three-dimensional Measurement in Microscopy*. Oxford: Bios Scientific Publishers.

Jefferies, R. P. S. and Jacobson, A. G. (1998). An episode in the ancestry of vertebrates: from mitrate to crown-group craniate. *Integr. Biol.* **I**, 115–132.

Kent, G. C. and Miller, L. (1997). *Comparative Anatomy of Vertebrates*. Dubuque: Wm. C. Brown Publishers.

Mallatt, J. (1984). Early vertebrate evolution: pharyngeal structure and the origin of gnathostomes. *J. Zool., Lond.* **204**, 169–183.

Marshall, P. T. and Hughes, G. M. (1980). *Physiology of Mammals and other Vertebrates*. Second edition. Cambridge: Cambridge University Press.

Michel, R. P. and Cruz-Orive, L. M. (1988). Application of the Cavalieri principle and vertical sections method to lung: estimation of volume and pleural surface area. *J. Microsc*. **150**, 117–136.

Nicol, J. A. C. (1960). *The Biology of Marine Animals*. London: Macmillan Press.

Orton, J. H. (1913). The ciliary mechanisms on the gill and the mode of feeding in amphioxus, ascidians and *Solenomya togata*. *J. Mar. Biol. Ass.* **10**, 19–49.

Perry, S. F. (1978). Quantitative anatomy of the lungs of the red-eared turtle, *Pseudemys scripta elegans*. *Respir. Physiol*. **35**, 245–262.

Perry, S. F. (1981). Morphometric analysis of pulmonary structure. Methods for evaluation and comparison of unicameral lungs. *Mikroskopie (Wien)* **38**, 278–293.

Perry, S. F. (1990). Recent advances and trends in the comparative morphometry of vertebrate gas exchange organs. In *Advances in Comparative Environmental Physiology*, vol. 6 (ed. R. G. Boutilier), pp. 45–71. Berlin: Springer.

Perry, S. F., Hein, J. and van Dieken, E. (1994). Gas exchange morphometry of the lungs of the tokay, *Gekko gecko* L. (Reptilia: Squamata: Gekkonidae). *J. Comp. Physiol.* B **164**, 206–214.

Rähr, H. (1979). The circulatory system of amphioxus (*Branchiostoma lanceolatum* (Pallas)). A light-microscopic investigation based on intravascular injection technique. *Acta Zool.* **60**, 1–18.

Rähr, H. (1981). The ultrastructure of the blood vessels of *Branchiostoma lanceolatum* (Pallas) (Cephalochordata). I. Relations between blood vessels, epithelia, basal laminae and 'connective tissue'. *Zoomorph.* **97**, 53–74.

Riisgard, H. U. and Svane, I. (1999). Filter feeding in lancelets (amphioxus), *Branchiostoma lanceolatum*. *Inv. Biol.* **118**, 423–432.

Rogers, E. (1989). *Wirbeltiere im Überblick. Eine Praktikumsanleitung*. Heidelberg: Quelle & Meyer.

Rolph, W. (1876). Untersuchungen über den Bau des *Amphioxus lanceolatus. Morph. Jb.* **2**, 86–164.

Romer, A. S. and Parsons, T. S. (1977). *The Vertebrate Body*. Philadelphia: W. B. Saunders Company.

Stach, T. (1998). Coelomic cavities may function as a vascular system in amphioxus larvae. *Biol. Bull.* **195**, 260–263.

Stach, T. and Eisler, K. (1998). The ontogeny of the nephridial system of the larval amphioxus (*Branchiostoma lanceolatum*). *Acta Zool*. **79**, 113–118.

Storch, V. and Welsch, U. (1999). *Kükenthal. Zoologisches Praktikum*. Heidelberg, Berlin: Spektrum Akademischer Verlag.

Webb, J. E. and Hill, M. B. (1958). The ecology of Lagos Lagoon. IV. On the reactions of *Branchiostoma nigeriense* to its environment. *Phil. Trans. R. Soc. Lond. B* **241**, 355–391.

Weibel, E. R. (1970/71). Morphometric estimation of pulmonary diffusion capacity. I. Model and method. *Respir. Physiol*. **11**, 54–75.

Weibel, E. R. and Knight, B. W. (1964). A morphometric study of the thickness of the pulmonary air–blood barrier. *J. Cell Biol.* **21**, 367–384.

Welsch, U. (1975). The fine structure of the pharynx, cyrtopodocytes and digestive caecum of amphioxus (*Branchiostoma lanceolatum*). *Symp. Zool. Soc. Lond*. **36**, 17–41.

Wolf, H. (1941). Über die Beeinflussung der Kreislauftätigkeit bei *Amphioxus lanceolatus*. *Pflügers Arch.* **244**, 736–748.

Young, J. Z. (1981). *The Life of Vertebrates*. Oxford: Oxford University Press.